*Proceedings of the International Conference on Applied Mechanical Engineering Research (IC-AMER2019)*
*NIT Warangal, India – May 02-05, 2019*
*Paper No. XXX (The number assigned when the papaer is accepted )*

# Experimental and Numerical Modelling of ECMM on Al 7075 T6 Alloy

K. Samson Praveen Kumar[a*] and Dr. G. Jayachandra Reddy[b]
[a]*Dep. of Mechanical Engineering, YVUCE Proddatur, Kadapa A.P, India, sp.mech@yogivemanauniversity.ac.in*
[b]*Principal and Head, Dep. of Mechanical Engineering, YVUCE Proddatur, Kadapa A.P, India, Jcr.yvuce@gmail.com*
*Corresponding author Email: ksamsonpraveen@yahoo.com

---

Electro Chemical Micro Machining (ECMM) is a non-traditional machining technique in the area of mechanical engineering. It is more essential to meet increasing demand of the industries from aero to medical where ECMM is the promising technique, since it has been growing popularity in various areas of applications. It offers various advantages that contain better precision and control, higher machining rate, short lead time and wide range of materials that are harder to machine. In the present study the optimal values and influence of process parameters like voltage, electrolyte concentration and frequency on diametrical overcut of machined micro hole during ECMM process while machining Al 7075 T6 alloy are presented, for this purpose a bare electrode (cathode) has been used. Later on, using optimum combination of process parameters the hole is drilled with insulated electrode. The ECMM process for drilling hole with bare tool and insulated tool are simulated to identify the effect of tip reaction on anode profile and stray current machined zone using COMSOL Multi-Physics V 5.3a software considering electric field, temperature field and fluid field, for deep understanding of the process. The results are validated with experimental results. The simulated predicted model is in superior conformity with experimental model.

***Keywords:*** Electrochemical micromachining (ECMM), Stray current machining, Multi-Physics, Modeling and Simulation

## 1. Introduction

In the current development the micro products has been rapidly increasing demand in the field of automotive, bio-medical, aerospace, biotechnology, optics, avionics industries and electronics [1] and the quantity materials which are difficult-to-machine like super alloys has considerably increasing because of their improved properties [2]. While machining such materials using conventional machining process a lot of issues like heat affected zone, tool wear, high surface roughness, thermal stress and mechanical forces are being occurring [3-5]. To overcome this issue various methods has been developed [7]. Electro chemical machining is one of such machine and removal of material in the range of microns is known as micro machining [6]. Electro Chemical Micro Machining (ECMM) is an anodic dissolution process where tool (cathode) and workpiece (anode) are locally suspended in the electrolyte [8]. The ECMM process works on the principle of Faraday's laws of electrolysis. The ECMM process is emerging to be assuring method because of its additional advantages [9-11]. Even though it is difficult to achieve machining accuracy and it becomes challenging. From the past information it is clear that the machining accuracy in the form of diametrical overcut is influenced by the tool used, the process parameters and stray current. Therefore, it has been drawn attention in design of tool, analyzes the various process parameters and stray current machining. In the ECMM process the disk shape tool tip is useful to reduce the taper during machining micro-hole [12]. The use of different tapered tool tips for machining micro-channels and micro-holes [13-14]. The effect of spherical tip of tool cathode has been investigated during machining micro-hole [15]. To avoid stray current influence on the surface and side walls [16]. All the authors above focused on the bare tool with different tool tip shapes. The electric field supply in the Inter Electrode Gap (IEG) using bare tool and insulated tool is shown in Fig. 1a and 1b. The researcher's approaches multi-physics model for prediction of process performance characteristics [17-19]. The ECM process was numerically simulated for steel (anode) using $NaNO_3$ (electrolyte) [20]. However, in the ECMM process various physical fields are involved (temperature, electrical, fluid, etc). With the effect of these physical fields the process parameters, structure and tool are significantly decides machining accuracy [21-22]. On the other hand, the

researcher focused only on the bare electrode and electrical field, ensuing in a clear inconsistence among simulation and experiment. For this reason, multi-physics analysis is necessary for ECMM process to precisely know the cause of the tool on the machining accuracy.

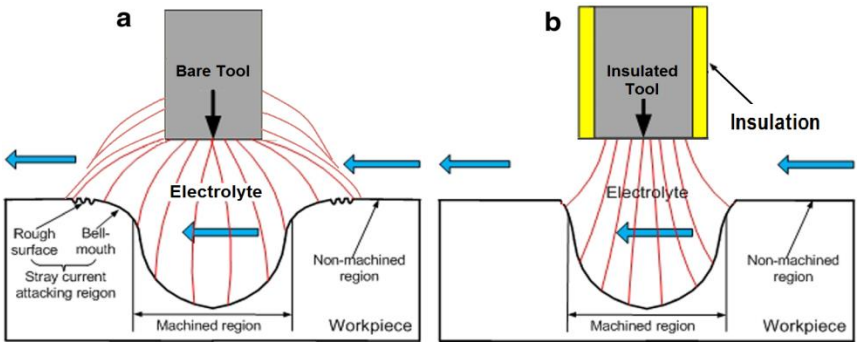


Fig. 1 The schematic of the ECMM process (a) Using bare tool with flat cathode tip (b) Using side-insulated tool with flat cathode tip.

The present investigation focuses on the optimum combination and influence of the process parameters (voltage, electrolyte concentration and frequency) on dimensional overcut with bare tool using ECMM process. Then find the influence of insulated tool on diametrical overcut with the optimum process parameters. After that a multi-physics model for ECMM process was developed to find the parametric and structural effects on the electrical field distribution, fluid and temperature fields. Finally validate the obtained results from simulations with the experimental results.

## 2. Experimental Procedure

The process parameters used to carry out machining are Voltage, Electrolyte concentration and Frequency which are considered as variables. The other parameters like current 0.8 A, feed rate 28.2 µm/s and duty cycle 60% are considered as constants. The tool diameter as 300 µm, Electrolyte as $NaNO_3$ and tool material as copper has been used to conduct the experiments. The corresponding values and levels of process parameters are chosen based on past information and preliminary experiments conducted are voltage (6, 8, 10) V, Electrolyte concentration (25, 30, 35) g/l and frequency (40, 50, 60) Hz respectively. The experimental work was designed based of $L_{27}$ Orthogonal Array method to perform micro hole on Al 7075 T6 of thickness 0.3 mm and size 20 mm X 20 mm using ECMM process, where the output of dimensional overcut is calculated by noting down the diameter of hole after machining for each trail. In this study the target is to have lower overcut. To achieve this optimization technique has to perform with the help of Taguchi analysis and ANOVA. After attaining the optimum combination of process parameters, machining has been done with insulated tool where the insulating material is PVC to study the dimensional overcut. After completion of experiments, the micro-hole entrance was examined with SEM.

## 3. Numeric Model

A two dimensional models were developed with the same machining conditions of experiments and simulated using COMSOL Multi-Physics. The ECMM model has several physical domains like electrical field, deformed geometry interface, fluid field and temperature field is set up to analyze the interactions between tool and workpiece. The modeled multiphysical fields coupling corelation is shown in the Fig. 3. The coupled model of the above fields can be interface the plysical fields in ECMM with the following assumptions. The ECMM process is assumed to be ideal i.e., the changes in composition of the electrolyte are negligible and the activation over potentials of the electrode responses are negligibly small, the reaction products of heat, bubbles, and ions are neglected, the model is isothermal, the thermal conductivity of the electrolyte is assumed to be constant and the fluid properties of the electrolyte are considered constant. In the electrolyte the

varyations of composition are ngligible as the electrode initiation overopotential are negligibly small. In the past simulations the side insulated layers [21-24], are simplified to one dimenstional electrically insulated limits. The researches shows the importance of insulated layers [25-26]. Therefore it is significantely consider to study the infulance of side insulated layer construction on the multi-physics.

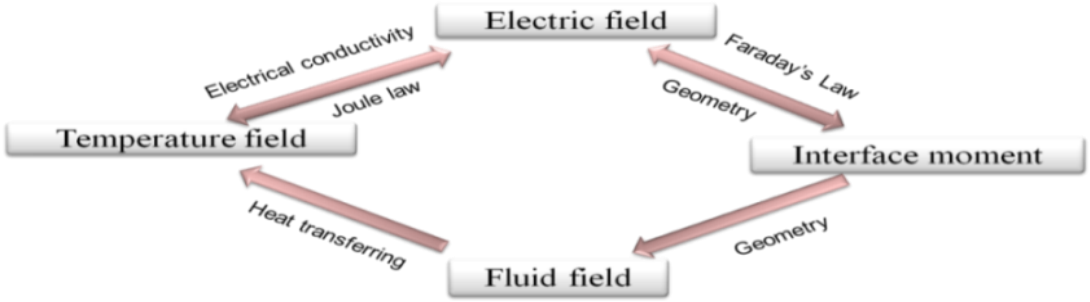


Fig. 3 Schematically illustration of the coupling corelation of the multiphysical fields

### 3.1. Geometry model

The two dimentional geometry model contains of 4 domains namely cathode, anode, electrolyte and insulation. The IEG intially maintained as 40 microns and the electrolyte flows from inlet right to outlet left. The geometry model was developed for ECMM process according to the experimentation as shown in Fig. 4.

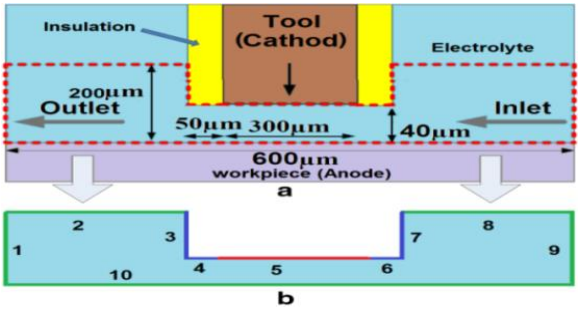


Fig. 4 Geometry model (a) The schematic of the electrolytic cell used in ECMM process (b) The developed geometry model

### 3.2. Physic

#### 3.2.1. Material Dissolution

The material dissolution was carry out together with the interface of electric current and deformed geometry models. The domain of the electrolyte was assigned to water from the material library and defined with an electric conductivity of 0.165 S/m according to the performed experimental investigations. The boundary conditions of the mode electric current according to Fig. 4 are listed in Table. 1. The ECMM follows the Faraday's law as functional principle for anodic dissolution of material due to electric potential Q. The material removed in volume V is calculated as.

$$V = \eta \, \mathrm{x} \frac{M}{\rho \, . \, z \, . \, F} \, \mathrm{x} \, \mathrm{Q} \qquad (1)$$

η is the current efficiency, M is the molar mass, F the Faraday constant, z the electrochemical valence of the material and ρ the density. The material removal velocity $\vec{v}_n$ in normal direction depends on the current density $\vec{j}_n$ in normal direction.

$$\vec{v}_n = \eta(J) \, \mathrm{x} \frac{M}{\rho \, . \, z_A \, . \, F} \, \mathrm{x} \, \vec{j}_n \qquad (2)$$

$$\eta(J) = \begin{cases} 1 \; for \; J > J_{min} \\ 0 \; for \; J \leq J_{min} \end{cases} \quad (3)$$

The current density $J_{min}$ was taken as 10 A/cm$^2$ according to past literature. Other paremters require to calculate errosion according to Eqs. (2) are current efficiency as 100%, molar mass as190894.3856 g/mol, vanency as 3, mass density as 2.81g/cm$^3$ and Faraday's constant as 9.65x104 C/mol.

### 3.2.2. Deformed Geometry

The deformed geometry interface can be used to study how physics changes in case the geometry shrinks by removal of material, Hear the geometry changes because of the some active physics interface available. The interface requires a domain selection and has to select the geometry shape order as 1 and mesh smoothening type as Laplace where the geomerty shape order controls the order of polynominals used for indicative of geometry shape in materual frame. The free displacement has to be activated where Lagrange-Eulerian (ALE) method shape function uses same order for mesh position in domains.

### 3.2.3. Non-Isothermal Electrolyte Flow

The non-isothermal laminar flow interface is used to simulate the couple between fluid flow and heat transfer and it combines the laminar flow and heat transfer in fluids.

#### a. Laminar Flow

The laminar flow interface has been solved with the incompressible laminar Navier- Stoke equation where the flowing velocity u can be expressed.

$$\rho \nabla(u) = 0 \quad (4)$$

$$\rho \frac{\partial u}{\partial t} + \rho(u\nabla)u = \nabla[-Pl + \mu(\nabla u + (\nabla u)^T)] + F \quad (5)$$

Where ρ is electrolyte density, p is the flud pressure and μ is the dynamic viscosity. The boundary conditions of the laminar flow according to Fig. 4 are listed in Table. 1. The normal in flow velocity is taken as 0.1 m/s, density of electrolyte is taken as 1908 kg/m$^3$, pressure as 1 atm and dynamic viscosity is taken as 00.00125 pa-s.

#### b. Heat Transfer in Fluids

When the current is passed through two elctrodes a resistive heating is generated kinown as Joul's heating which increases temperature in the electrolyte and thus increases the conductivity of electrolyte. The boundary conditions for heat transfer in fluids model according to Fig. 4 are listed in Table. 1. The boundary 5 is defined as heat flux and is approximately taken 106 w/m$^2$[21].

Table. 1. Boundary conditions of multi-physics model

| Boundary settings of electric model | | | |
|---|---|---|---|
| Boundary condition | Electric potential | Electrical insulation | Ground |
| Boundary No. | 5 | 1,2,3,4,6,7,8,9 | 10 |
| Setting | $U_0$ = 6V | n.j = 0 | $U_0$ = 0 |
| Boundary settings for fluid model | | | |
| Boundary condition | Inlet | Out let | No slip wall |
| Boundary No. | 9 | 1 | 2,3,4,5,6,7,8,10 |
| Setting | u = - $u_{in}$ n | P = 1 atm | u = 0 |

| Boundary settings for heat transfer model | | | |
|---|---|---|---|
| Boundary condition | Heat flux | Thermal insulation | Temperature reference |
| Boundary No. | 5 | 1,2,8 | 3,4,6,7,9,10 |
| Setting | $-n \cdot q = d_z q_0$ ($q = -d_z k\nabla T$) | $-n \cdot q = 0$ | $T=T_0$ |

Hear for the simulation of heat transfer in fluids the results of laminar flow were used coupled with primary current model. The heat transfer in fluids model uses the following Eqs. (6)

$$\rho C_p \left(\frac{\partial T}{\partial t} + u\nabla T\right) = \nabla(k\nabla T) + Q \quad (6)$$

Where $C_p$ is the specific heat at constant pressue and is taken as 1655 J/(kg-K), u is velocity of electrolyte 0.1 m/s, T is the temperature 273.15 K and Q is the heat source which come from electric current.

### 3.2.4. Mesh

An unstructured mesh has been used to the geometry. To atain this mesh, user-defined mesh has been chosen and in the settings minimum and maximum element size are 50 μm and 500 μm respectively. Then a free tringula mesh was chosen in that for size1 the minimum and maximum element sizes are 1 μm and 50 μm has been assigned to boundary 5 and for size2 the minimum and maximum element sizes are 1 μm and 50 μm has been assigned boundary 10.

## 4. RESULTS AND DISCUSSION

### 4.1. Experimental Results

The experimental results are analysed throuth Taguchi Analysis and ANOVA using statistical software, MINITAB 18 are listed in the Table. 2 and Table. 3. From Table. 3 the factor voltage has the desired level is 1, because of the over cut value is minimum. Similarly, the desired levels for electrolyte and frequency are 2 and 1 respectively. Therefore, the optimal process parameters are voltage as 6V, electrolyte as 30 g/l and frequency as 40 Hz.

Table. 2. Mean effective response (smaller the better)

| Level | Voltage | Electrolyte | Frequency |
|---|---|---|---|
| 1 | 69.11 | 91.67 | 101.78 |
| 2 | 95.78 | 86.78 | 113.22 |
| 3 | 172.11 | 158.56 | 122.00 |
| Delta | 103.00 | 71.78 | 20.22 |
| Rank | 1 | 2 | 3 |

The parameters which significantly influence the output characteristics are with p-value ≤0.05 under 95% confidence levels. It is clear from the Table. 3, where the voltage is the most influencing factor and electrolyte is also significantly influence factor.

Table. 3 Analysis of Variance results

| Source | DF | Adj SS | Adj MS | F-Value | P-Value |
|---|---|---|---|---|---|
| Voltage | 2 | 4.0570 | 2.0285 | 10.48 | 0.001 |
| Electrolyte | 2 | 1.7149 | 0.8574 | 4.43 | 0.026 |
| Frequency | 2 | 0.2129 | 0.1065 | 0.55 | 0.585 |
| Error | 20 | 3.8699 | 0.1935 | | |
| Total | 26 | 9.8547 | | | |

The effect of various process parameters during machining are shown in the Fig. 7 below and it is clear that the over cut increases with the increase of voltage as the ions increases in the electrochemical cell which increases the material removal and also increases the current flow through IEG. For the higher values of current there will be the more current density which leads to higher removal of material at the edges of hole as a result higher over cut. Therefore, lower values of voltage is preferable for minimum over cut,

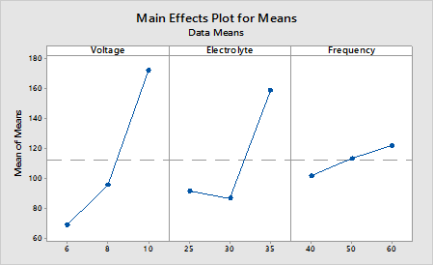


Fig. 7 Effect of various process parameters

The influence of electrolyte concentration on over cut is when it increases over cut reduces at moderate values and increases further at higher concentration because of the increase of ions association in the machining zone. A higher ion concentration improves the current density in the IEG resulting in increasing overcut. Thus the moderate value of electrolyte concentration is preferable. The influence of frequency is not much higher when compared to voltage and electrolyte concentration. Hear as the frequency increases over cut also increases.

## 4.2. Simulation Results

### 4.2.1. Material Dissolution

The simulation results for material dissolution of bare tool and insulated tool for current density distribution and electrolyte potential distribution are shown in Fig. 8. Obviously, it is clear that the insulated tip is helpful to restrict the effect of stray current in the IEG. The arrows in Fig. 8 (a) bare tool and (b) insulated tool shows the moment of ions which clearly indicating that the ions are moving more in case of bare tool simulation than insulated tool simulation. The insulated layer confined the current attack on more localized area, which conforms the reducing of stray corrosion and overcut in ECMM process.

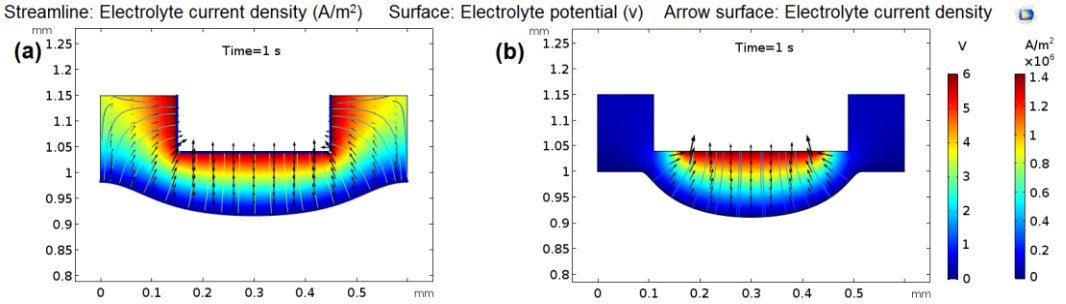


Fig. 8 Current density and electrolyte potential distribution (a) bare tool (b) insulated tool

The effect of bare tool and insulated tool on anode profile and current density distribution was investigated hear, as shown in Fig. 9. The light gray shaded rectangle shows position of the tool. Fig. 9 (a) shows that when bare tool is chosen, the distribution of current density is evidently dispersed an extensive range of the nearby surface go through stray current of the machined region. The removal of material from this region is known as stray current attacking [27], which generally caused bell-mouth profile [28-29]. On the other hand Fig. 9 (b) shows, when insulated tool is used, the current density distribution focuses towards the machined zone. The current spreading from cathode can be limited by the insulated layer and restricted to a lesser region.

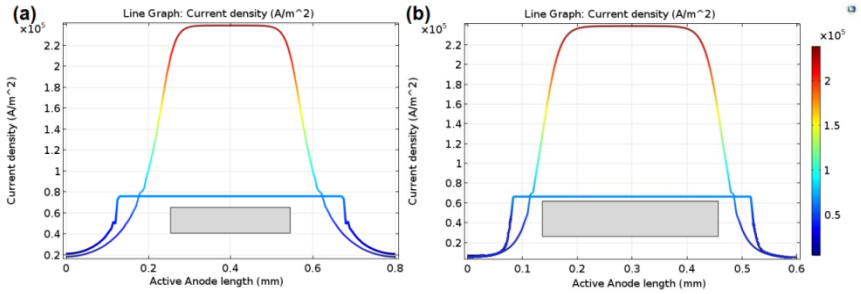


Fig. 9 Current density distribution and anode profile of (a) bare tool (b) insulated tool

### 4.2.2. Non-Isothermal Laminar Flow

The non-isothermal laminar flow simulation starts with independent simulation of the laminar fluid flow. The outcome of this simulation is depending on the flow field characterization through velocity field. Fig. 10 shows the electrolyte velocity magnitude (a) with bare tool and (b) with insulated tool. It is clear from Fig.10 (a) that the velocity is more in the machined zone because of the formation of bell-mouth and in case of insulated tool the velocity is comparatively less.

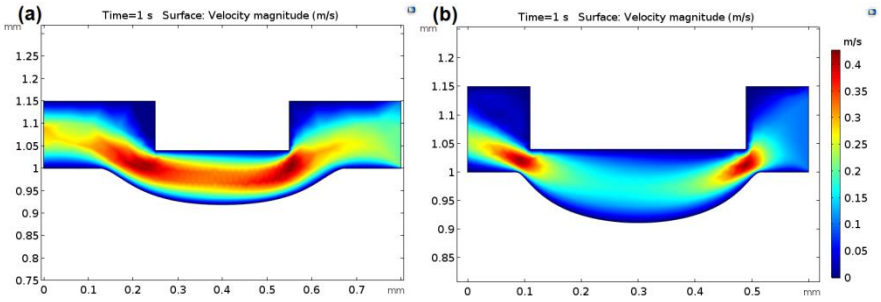


Fig. 10 Velocity magnitude (a) with bare tool and (b) with insulated tool

The velocity profile has an influence on temperature distribution, where the temperature occurs because of Joul's heating, conduction and convection. Fig. 11 shows the temperature distribution simulation and it is clear that the temperature distribution simulation of the electrolyte follows the velocity profile computation. Comparing Fig. 11 (a, b) with (c, d) it can be observe that the distribution of temperature with bare tool tip is extremely asymmetric.

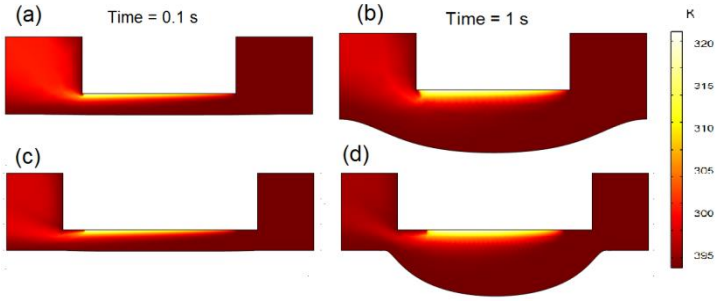


Fig. 11 Temperature distribution of bare tool (a) at time = 0.1 s (b) at time = 1 s and insulated tool (c) at time = 0.1 s (d) at time = 1 s

With insulated tool tip the distribution of temperature turn out to be more symmetric because of the insulated layer restricting effect on the electrolyte convection. In addition, comparing Fig. 11(a) and (b) it can be observed that with the increasing of time in bare tool tip, the distribution of temperature becomes more symmetric. The temperature increases to

some extent and presents even trends only in case of insulated tool tip. Therefore, to obtain high machining accuracy a stable environment temperature is predicated.

## 5. EXPERIMENTAL VERIFICATION

The experiments for both the bare tool and insulated tool of the optimum combination process parameters were conducted for compression. The simulation results are qualitatively compared with experimental results. The surface quality and entrance shape are used to estimate the machine accuracy. Figure 12 shows the SEM images of the machined holes at entrance. As shown in Fig 12 (a) which is machined with bare tool clearly show evidence of a stray current attack region, entrance shape is fairly asymmetric and has bell-mouth shape. Insulated tool machined hole is shown in Fig. 12 (b) which is clearly evident for no stray current attack. The experimental results, thus well agree with the simulation results of a more intense current density distribution and better non-isothermal fluid flow using insulated tip tool.

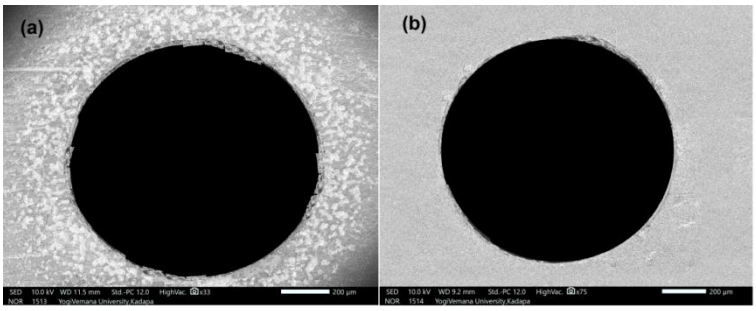


Fig. 12 SEM images of machined hole with (a) bare tool (b) insulated hole

## 6. CONCLUSION

In this paper, an experimental investigation has been carried out to know optimal combination levels of process parameters using Taguchi analysis method and also to find the influence of process parameters using ANNOVA method during machining micro-hole on Al 7075 T6 alloyon diametrical overcut using ECMM process. It has been made an attempt to model and simulate the ECMM process for optimum combination of process parameters with bare tool and insulated tool using COMSOL Multi-physics V5.3a software. Based on the experimental and simulated results and analysis, the following conclusions can be made.

1. The optimal combination levels of process parameters were voltage of 6V, electrolyte concentration of 30 g/l and frequency of 40 Hz.
2. From ANNOVA analysis the most significant process parameter that influences lower OC is voltage and electrolyte is also considerably influence factor.
3. The multi-physics simulation results very closely agree with the experimental results. Therefore, multi-physic can be selected as substitute to the costly trial and error method.
4. The simulated and experimental results propose the use of insulated tool which is able to produce high quality hole without any stray current attacking zone, good from minimum overcut and accuracy.

### ACKNOWLEDGEMENT

The authors thank the management of Sona College of Technology (Autonomous Institution), Salem, Tamil Nadu for the encouragement and support. The authors also thank Dr. P. Suresh in-charge for CNM/CMM lab, Dep. Of Mechanical Engineering, Sona College of Technology, Salem, Tamil Nadu for his supervision and allowing me to utilize the Micro ECM setup with pulse rectifier and optical microscope.

## REFERENCES


[1] K. P. Rajurkar, G. Levy, A. Malshe, M. M. Sundaram, J. McGeough, X. Hu, R. Resnick, and A. DeSilva, Manufacturing Technology, vol. 55, no. 2, pp. 643-646, December (2006)

[2] E.A. Ott, J.R. Groh, A. Banik, I. Dempster, T.P. Gabb, R. Helmink, X. Liu, A. Mitchell, G.P Sjoberg, and A. Wusatowska-Sarnek, The Minerals, Metals & Materials Society (2010)

[3] T. Muthuramalingam, B. Mohan, Journal Archives of Civil and Mechanical Engineering, 15 (1): 87-94, (2015)

[4] H. R. Shi, Journal of Material Processing Technology, 209 (6): 2831-2837,(2009)

[5] H. A. Se, H. R. Shi, K. C. B. Deox, Precision Engineering, 28 (2): 129-134,(2004)

[6] B. Bhattacharyya and J. Munda, Journal of Materials Processing Technology, vol. 140, no. 1, pp. 287-291, September (2003)

[7] Ryu, S.H, Journal of Material Processing Technology, Vol. 209, No. 6, pp.2831–2837, (2009)

[8] McGeough JA, Chapman and Hall, London (1974)

[9] B. Bhattacharyya, J. Munda, M. Malapati, International Journal of Machine Tools & Manufacture, 1577–1589, doi:10.1016/j.ijmachtools, (2004).

[10] Malapati, M. and B. Bhattacharyya, Materials and Manufacturing Processes, 26, 1019-1027, (2011)

[11] Spieser, A. and A. Ivanov, The International Journal of Advanced Manufacturing Technology, 69, 563-581, (2013)

[12] Kim BH, Na CW, Lee TS, Choi DK, Chu CN, CIRPAnnals-Manuf Technol 54(1):191–194, (2005)

[13] Choshal B, Bhattacharyya B, Precis Eng 38:127–137, (2014)

[14] Choshal B, Bhattacharyya B, Journal of Mater Process Technol 222:410–421, (2015)

[15] Liu Y, Zhu D, Zeng YB, Yu HB, Int J Adv ManufTechnol 55:195–203, (2011)

[16] Li Y, Yang YF, Peng LQ, Sensors Actuators 108:144–148, (2003)

[17] Matthias Hackert-Oschatzchen, Michael Kowalick, and Gunnar Meichsner, Proc. COMSOL Conference, Milan, Italy (2012)

[18] Van Tijum R, and Pajak P.T, Proc. COMSOL Conference, Hannover, Germany (2008)

[19] Xiaolong Fang, Ningsong Qu, and Yudong Zhang, Journal of Materials Processing Technology, vol. 214, p. 36, (2014)

[20] Deconinck D, Van Damme S, and Deconinck J, Electrochimica Acta, vol. 60, p. 321, (2012)

[21] Deconinck D, Van Damme S, Albu C, Hotoiu L, Deconinck J, Electrochim Acta 56: 5642–5649, (2011)

[22] Wu J, Wang H, Chen X, Cheng P, Ding G, Zhao XL, Huang Y, Electrochim Acta 75: 94–100, (2012)

[23] Hourng LW, Chang CS, Journal of Appl Electrochem 24:1170–1175, (1994)

[24] Sun CH, Zhu D, Li ZY,Wang L, Finite Elem Anal Des 43:168–172, (2006)

[25] Datta M, Landolt D, Electrochim Acta 45:2535–2558, (2000)

[26] Chen XL, Qu NS, Li HS, Guo ZN, Precis Eng 39:204–211, (2015)

[27] Jain VK, Kanetkar Y, Lal GK, Int J Mach Tools Manuf 26:527–536, (2005)

[28] Wang W, Zhu D, Qu SN, Huang SF, Fang XL, J Mater Process Technol 210:238–244, (2010)

[29] Kawanaka T, Kato S, KuniedaM, Procedia CIRP 13:345–349, (2014)